J Appl Electrochem (2009) 39:1963–1973
DOI 10.1007/s10800-009-9906-2

ORIGINAL PAPER

Model calculations to optimise multi-cathode flow through electrolysers: direct cathodic reduction of C.I. Sulphur Black 1

Thomas Bechtold · Aurora Turcanu · Heiko Brunner · Wolfgang Schrott

Received: 24 January 2009 / Accepted: 14 April 2009 / Published online: 2 May 2009

Abstract A laboratory cell equipped with multiple porous electrodes connected electrically in parallel and hydrostatically in series was used to reduce dispersed Colour Index (C.I.) Sulphur Black 1 to synthesise C.I. Leuco Sulphur Black 1. At higher cell current bipolar effects limit the maximum thickness of a porous cathode element. A mathematical model has been established to estimate the maximum thickness of a cathode element. The cell voltage can be calculated using a simple resistor network. The presented model calculations permit optimisation of a cell with multiple porous electrodes with regard to dimensions, cell costs and energy consumption. A multi-cathode cell, equipped with 10 cathodes for a total cell current of 10 A, was used to study production of highly concentrated C.I. Leuco Sulphur Black 1 solutions. Compared to chemical reduction, dyeing behaviour was found to be independent of reduction method used.

Keywords Sulphur dye · C.I. Sulphur Black 1 · Cathodic reduction · Multi-cathode electrolyser · Porous electrodes · Three-dimensional electrode

List of symbols

ΔU_i	Potential difference in catholyte between front and back side of a cathode unit (V)
ΔU_{max}	Maximum permitted difference in cathode potential between front and back side of a three-dimensional cathode unit (V)
d_i	Thickness of the three-dimensional cathode unit (cm)
A	Front area of the cathode (cm^2)
ω	Open part of cathode area A (%)
κ	Conductivity of the catholyte (mS cm^{-1})
i_d	Diffusion limited current density (mA cm^{-2})
I_c	Total cell current (A)
i	Position of electrode ($i = 1$ first and $i = n$ last cathode)
n	Number of cathode units in multi-cathode cell
I_i	Current transported through porous cathode i (A)
I_1^*	Current fed into cathode unit 1
I_i^*	Current fed into cathode unit i
I_n^*	Current fed into cathode unit n
L_i	Number of layers forming one cathode unit
C_1	Coefficient transferring the geometric area of an electrode layer into surface area
C_2	Thickness of a single layer of electrode material (steel fabric) (cm)
U_1	Cell voltage of cathode unit 1 (V)
U_i	Cell voltage of cathode unit i (V)
U_n	Cell voltage of cathode unit n (V)
R_0	Resistance of catholyte/membrane and anolyte, anode reaction and anode (Ω)
R_i	Resistance of catholyte between two neighbouring cathode units (Ω)
R_z	Resistance of a cathode unit including cathodic reaction and contribution of cathodic overvoltage (Ω)
R_{cell}	Contribution of cathode, anode and cation-exchange membrane to cell resistance (Ω)

T. Bechtold (✉) · A. Turcanu
Research Institute for Textile Chemistry and Textile Physics, Leopold-Franzens University Innsbruck, Hoechsterstrasse 73, 6850 Dornbirn, Austria
e-mail: Thomas.Bechtold@uibk.ac.at

H. Brunner · W. Schrott
DyStar Textilfarben GmbH&Co Deutschland KG, 65926 Frankfurt a. M., Germany

1 Introduction

The annual production of C.I. Sulphur Black 1 (SB1) worldwide exceeds 80.000 tons. SB1 is believed to contain polymeric phenothiazine groups as shown in Scheme 1 [1].

Sulphur Black 1 is a so-called bake-pot sulphur dye, which is synthesised by baking 2,4-dinitro-chloro-benzene with Na_2S and S_x. The final step in the dyestuff synthesis is the oxidation of the reduced dye by air oxygen to precipitate SB1 in its oxidised form. The crude dyestuff then is filtered off and by-products are removed by rinsing with water.

Highly concentrated solutions of Leuco Sulphur Black 1 are the preferred commercial form in the industry, thus the oxidised filter cake has to be reduced in alkaline solution, mainly by means of sodium sulphide or glucose [2–6]. Chemical reducing agents used at present, cannot be regenerated, thus besides costs for chemicals, environmental problems, e.g. due to toxicity or high chemical oxygen demand in the waste water, become more and more important [5, 7]. A promising strategy to replace the reducing agents is direct cathodic reduction of SB1 [8, 9].

Sulphur Black 1 can undergo several reduction/oxidation steps in solution (Scheme 1). A dyestuff molecule in its reduced state is able to carry a reduction capacity of up to six equivalents from the cathode into the dyebath, and thus, can take over the function of a redox mediator [1]. In the literature, direct cathodic reduction of crude SB1 has been reported. Diluted solutions of the reduced dye successfully were used for continuous pad-steam dyeing, exhaust dyeing and denim yarn dyeing [10–14]. For production of a commercial liquid dyestuff formulation, the dye has to be reduced cathodically at very high concentration. In the dyehouse, the concentrated product then is added in required amount to the dyebath.

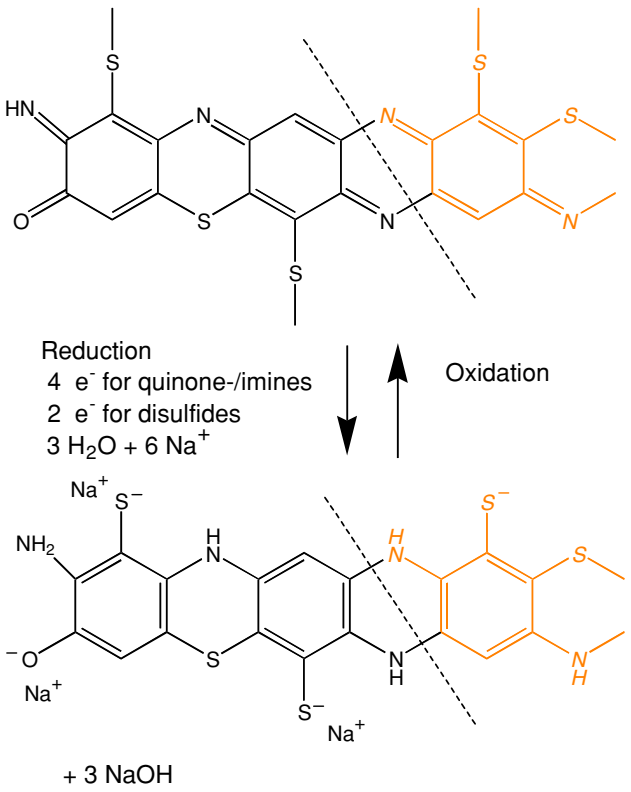

Scheme 1 Representative structure of C.I. Sulphur Black 1 (SB1) and reduction reaction to Leuco Sulphur Black 1

Due to limited concentration of cathodically active species and rather high molecular weight, the cathodic reduction of SB1 proceeds only at rather low current density. Thus, electrolysers with high electrode surface-to-volume ratio have to be used. Since the reduced dyestuff is soluble in alkaline solution, cell designs with three-dimensional flow through cathodes can be applied without fear of filtration.

Different designs for three-dimensional electrodes have been described in the literature, such as porous electrodes, packed bed electrodes and fluidized bed electrodes [15–20]. A wide range of materials have been tested for possible application in three-dimensional electrodes, for example, foamed nickel structures for cathodic electrohydrogenation reaction, electrodeposited PbO_2 for the anodic oxidation of cyanide, or activated carbon fibres for ground water purification [21–23].

For an efficient application of three-dimensional electrodes, the mass transfer and current distribution have to be optimised [24–26]. Current density distribution in packed bed electrodes is not uniform and depends on a number of factors, for example, conductivity of both electrolyte and porous electrode material. Electrode thickness and porosity of the electrode, conductivity of the electrode material and applied current density have to be optimised for a certain electrolyte conductivity and electro-active system concentration. In a three-dimensional electrode, a limited depth of a three-dimensional structure is involved into the electrochemical process, which restricts the maximum surface-to-volume ratio of a cell concept [27]. A detailed analysis of a three-dimensional packed bed cell for metal recovery has been presented in literature [28–31]. Modelling of current density and current efficiency of a packed bed electrochemical reactor for organic synthesis of glyoxylic acid has been reported in the literature to be in good agreement with experimental data [32].

Use of additional equipotential current feeders into porous electrodes to achieve more even current distribution in a three-dimensional electrode also has been proposed in the literature [33]. A strategy to achieve equal current distribution in a three-dimensional electrode is the use of multiple porous electrodes connected electrically in parallel and

hydrostatically in series [10, 12, 13, 34–37]. For low cell currents, an individual adjustment of electrode potential can be achieved by external resistors [38]. In a variation, the electrode is built up from several layers of expanded metal, the layers being connected internally by appropriate resistors [39].

Due to the advantage of multiple electrode cells to operate at low current density, such cells have been proposed for use in water treatment processes [40].

In corrosion studies, the concept of using two potentiostats sharing a common auxiliary electrode has been used to adjust different potentials to specimen electrodes [41]. The high potential drop in the electrolyte makes potential measurement difficult at higher cell current and special techniques have to be applied to control the electrode potential [42]. Thus, galvanostatic electrolysis is preferable. Such cells have been tested in full scale application for dyeing with indigo for cell current up to 1,000 A [43]. Above a critical cell current the individual cathodes in such electrolysers begin to exhibit bipolar reaction, which lowers efficiency and performance of the system [34].

In literature, only little information is available on about the proper design and performance of a multi-cathode electrolyser equipped with flow through electrodes [34, 35]. Thus, cell design is based mainly on empirical work and experimental optimisation. Electrolyte composition and cathode materials are defined by the process conditions, thus optimisation activities concentrate on the geometry of the three-dimensional electrode stack.

A mathematical formulation to estimate the maximum cathode thickness in a multi-cathode electrolyser as a function of process parameters is presented in this study. Such model calculations are of particular importance, when a higher number of three-dimensional electrodes, e.g. 10 cathode units are combined to a multi-cathode stack and the current transported in the electrolyte through a porous electrode exceeds by far the current of an individual three-dimensional electrode. A resistor network model to calculate the cell voltage of the individual electrodes in the cathode stack also is presented in this article.

The application of a pilot scale multi-cathode electrolyser to prepare reduced C.I. Sulphur Black 1 by direct cathodic reduction is used as representative example. In the multi-cathode electrolyser, a number of steel fabric electrodes were combined to a three-dimensional cathode stack, each cathode being connected to a separately adjustable power supply and a common anode.

The cell was used to produce concentrated solutions of Leuco Sulphur Black 1 starting with the oxidised crude filter cake. The reduced catholyte then was tested in exhaust dyeing experiments. For comparison, reference dyeings with use of sulphide based reducing agents were also prepared.

2 Experimental

2.1 Chemicals

Crude filter cake C.I. Sulphur Black 1 (SB1) was used as delivered (water containing solid, 63.7% solids in experiment nos. V1, V2, V3 and V5, and 60% solids in experiment no. V4, DyStar, Frankfurt a.M., Germany). Primasol®NF (Alkylphosphate, BASF AG, Ludwigshafen a.R. Germany) was used as wetting agent. Technical grade NaOH was used as ground electrolyte. Analytical grade $K_3[Fe(CN_6)]$ was used for determination of the reducing equivalents in the catholyte. All chemicals used in dyeing experiments were technical grade: wetting agent (Leonil® KS, Clariant, Basel, Switzerland), sodium polysulphide (Stabilisal®S fl) and sodium sulphide (Sulfhydrate® F 150) (DyStar Frankfurt a.M., Germany), NaCl, NaOH (50% w/w aqueous solution), H_2O_2 (35% w/w) and acetic acid (80% w/w).

2.2 Laboratory scale multi-cathode electrolyser

A multi-cathode flow through electrolyser equipped with 10 three-dimensional cathodes was used for the reduction experiments. The cathode stack was built up from 10 isolated cathode units attached to separately adjustable power supplies and connected to a common anode. Before the electrolyte flow entered into the three-dimensional electrode stack, the solution had to pass through two additional cathode units that were not connected electrically and served as pre-filter. Anolyte and catholyte were separated by a cation-exchange membrane (Thomapor MC-3470). Relevant data of cell and electrodes are given in Table 1. The individual three-dimensional cathodes were manufactured form two layers of stainless steel fabric (Haver & Boecker, Oelde, Germany). The catholyte flow was parallel to the current flow through the porous cathode stack. A general scheme of the electrolyser is given in Fig. 1.

The redox potential in the catholyte was measured with a Pt electrode versus a Ag/AgCl, 3 M KCl reference (potentiometer Metrohm 654 pH-meter, Herisau, Switzerland). The pH in the catholyte was measured with a glass electrode and a potentiometer (Hamilton-flush-trode, Orion 720A, Orion Research Inc. Boston, MA).

At the beginning of an electrolysis experiment, the anolyte compartment was filled with 1.5 dm^3 of 1 M NaOH. Dependent on the total charge flow concentrated NaOH (19.2 M) was added to the anolyte to maintain alkali concentration at 1 M NaOH.

The catholyte compartment was filled with an initial volume of 0.075 M NaOH (Table 2) and 1 g dm^{-3} wetting agent was added. Electrolysis was performed as galvanostatic process with a total cell current between 5 and 20 A.

Table 1 Technical data of the laboratory scale electrolyser and general experimental conditions

	Experimental parameter	Symbol	Dimension
Cathode	Geometric area of a cathode unit	A	400 cm^2 (20 × 20 cm^2)
	Surface area of cathode unit		0.19 m^2 (20 × 20 × 2 × 2.4[a] cm^2)
	Number of layers fabric	L_i	2
	Thickness of two layered cathode unit	d_i	0.08 cm
	Number of cathodes	n	10
	Total surface area of 10 cathode units		1.9 m^2
Material	Fabric, plain weave		Steel 1.4404
	Wire diameter		0.02 cm
	Open distance between wires		0.0315 cm
	Open area	ω	37%
	Factor surface/geometric area	C_1	2.4*
	Thickness per layer fabric	C_2	0.04 cm
	Mass per area		0.99 kg m^{-2}
Insulation	Fabric, plain weave		Polyethylene
	Wire diameter		0.03 cm
	Open distance between wires		0.15 cm
Catholyte	Volume		Max. 12 dm^3
	Composition		Alkaline dyestuff solution
	Catholyte flow through electrode stack		Max. 20 dm^3 min^{-1}
Anode	Material		Pt-mixed oxide coated titanium
	Geometric area		0.04 m^2
Anolyte	Total volume		1.5–2.0 dm^3
	Composition		1 M NaOH
Cell current	Total current	I_c	1–10 A
	Cathodic current density		0.5–5 A m^{-2}

[a] Factor to transform geometric area of steel wires in fabric into surface area

During electrolysis solid SB1 was added to the catholyte in portions.

Dyestuff reduction was monitored by redox titration of the reducing equivalents in the catholyte. A defined volume, e.g. 1.25 ml catholyte was added to a 50–60 °C warm mixture of 30 ml distilled water and 6 ml 1 M NaOH. Redox titration with 0.1 M $K_3[Fe(CN)_6]$ then was performed at 50–60 °C under an inert gas atmosphere using a titroprocessor equipped with a Pt redox electrode and Ag/AgCl, 3 M KCl reference (Orion 960 autochemistry system, Boston MA).

Relevant experimental conditions of the electrolysis experiments are shown in Table 2.

2.3 Dyeing procedure and reference dyeings

In prolongation of experiment V4, a concentrated solution of SB1 was prepared and tested in dyeing experiments. Dyeings were performed with two repetitions in a laboratory dyeing apparatus (Mathis Labomat BFA-8/16, Werner Mathis AG Niederhasli, Zürich, Switzerland). A 10 g sample of bleached knitted cotton fabric was dyed in 100 ml dyebath containing 2 g dm^{-3} wetting agent (Leonil® KS), 5 ml dm^{-3} polysulphide (Stabilisal®S fl), 20 ml dm^{-3} sodium sulphide (Sulfhydrate® F 150), 30 g dm^{-3} NaCl and 2 ml dm^{-3} NaOH (solution 50% w/w).

An amount of 10–25 g dm^{-3} cathodically reduced dyestuff was used in the dyebath. In case of reference dyeings, 10–15 g dm^{-3} Cassulfon Carbon® CMR (DyStar Frankfurt a.M., Germany) was used.

The textile sample was put into the dyebath at room temperature. The dyeing vessels were closed and heated to 50 °C with a heating rate of 2.5 °C min^{-1}, and from 50 °C to 95 °C with 1.8 °C min^{-1}. After 45 min dyeing time at 95 °C, the bath was cooled to 70 °C and the samples were rinsed in cold soft water. Oxidation of the dyeings was performed in 15 min at 70 °C in a bath containing 1% of sample weight H_2O_2 (35% w/w) and 2% of sample weight acetic acid (80% w/w). Following rinses in cold water, 80 °C water and cold water, the samples were line-dried.

CIE-Lab values of the dyeings were measured with a tristimulus colorimeter (Minolta Chroma-Meter CR 210, geometry $d/0°$, sample diameter 50 mm, illuminant D65). L^* corresponds to the brightness (100 = white, 0 = black), a^* to the red–green coordinate (positive sign = red, negative sign = green) and b^* to the yellow–blue coordinate (positive sign = yellow, negative sign = blue).

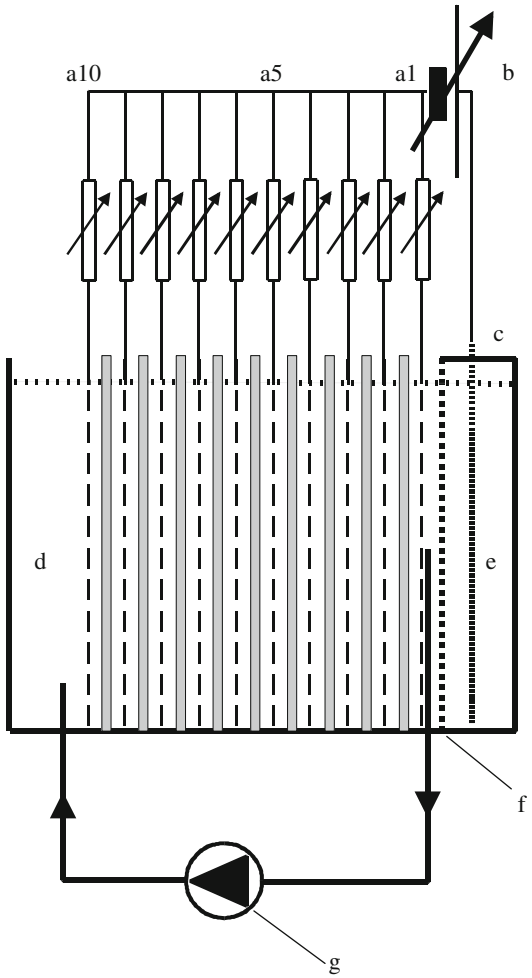

Fig. 1 Scheme of the multi-cathode cell including catholyte circulation and current supply. a_1 cathode 1, a_5 cathode 5, a_{10} cathode 10, *b* current supply, *c* anode, *d* catholyte, *e* anolyte, *f* cation-exchange membrane and *g* catholyte circulation

3 Results and discussion

3.1 Calculation of critical thickness of cathodes in a multi-cathode electrolyser

Cells equipped with multiple three-dimensional electrodes connected parallel electrically and in series hydrostatically offer high surface-to-volume ratio with regard to the active electrode area [34–36]. In the presented application, a multi-cathode electrolyser with porous steel fabric cathodes was used. The cathode stack was built up as combination of 10 isolated three-dimensional cathode units supplied by individual current sources, connected to a common counter electrode (Fig. 1).

The current density distribution in single three-dimensional electrodes can be calculated using mathematical models given in literature [24–31]. In a simplified approach, the ohmic drop in the electrolyte solution inside the porous matrix will cause lowering of current density with increasing electrode depth, which limits the active depth of a porous electrode.

In the tested multi-cathode electrode, 10 cathodes were combined to one electrode stack. In the three-dimensional cathode nearest to the anode, an ohmic drop ΔU_i of considerable magnitude is caused by the current flow in the electrolyte due to charge transport from other cathodes to the rear of the first cathode. A schematic presentation of the ohmic potential difference is shown in Fig. 2.

In Fig. 2, the voltage drop ΔU_i through a three-dimensional cathode, occurring in the catholyte is shown schematically. The voltammogram of SB1 recorded in a flow cell also is shown in Fig. 2 and side reactions are indicated, which occur, when ΔU_i exceeds the potential difference of the diffusion limited current plateau ΔU_{max}. With increasing cell current I_c, the potential difference in a cathode ΔU_i exceeds the potential difference of the diffusion limited current plateau ΔU_{max}. With $\Delta U_i > \Delta U_{max}$, the three-dimensional electrode begins to work in bipolar mode and side reactions will occur. In the case of cathodic SB1 reduction part of the three-dimensional electrode will produce hydrogen from water reduction, while to the rear of the cathode the reduced dyestuff will be reoxidised. In this case, insoluble reoxidised SB1 will filter into the porous electrode and the risk of electrode plugging by filtration of dispersed dyestuff appears. The ohmic ΔU_i exceeds the effects due to the current I_i^* of the electrode itself by far. This potential difference ΔU_i in the electrolyte limits the thickness of a three-dimensional electrode. When

Table 2 Conditions of electrolysis experiments: catholyte volume at begin of electrolysis, NaOH concentration at begin and end of electrolysis, concentration of SB1 in catholyte (crude product, dry dyestuff), cell current *I*, full charge flow *Q*, redox potential in catholyte *E*, temperature *T* and pH of catholyte

No.	Catholyte vol.	NaOH		Conc. SB1		I_c (A)	*Q*	*E*	*T* (°C)	pH
	Begin (dm^3)	Begin (mol dm^{-3})	End (mol dm^{-3})	Crude (g kg^{-1})	Dry (g kg^{-1})		End (Ah)	End (mV)		
V1	10	0.075	0.466	80	51	10	105	−618	21–36	12.3–12.5
V2	10	0.105	0.444	160	102	10	90.8	−599	21–32	12.1–12.5
V3	3.4	0.075	0.706	252	161	5	57.5	−521	24–32	12.4–12.6
V4	4	0.075	1.148	190	114	5/10	115	−607	28–35	–

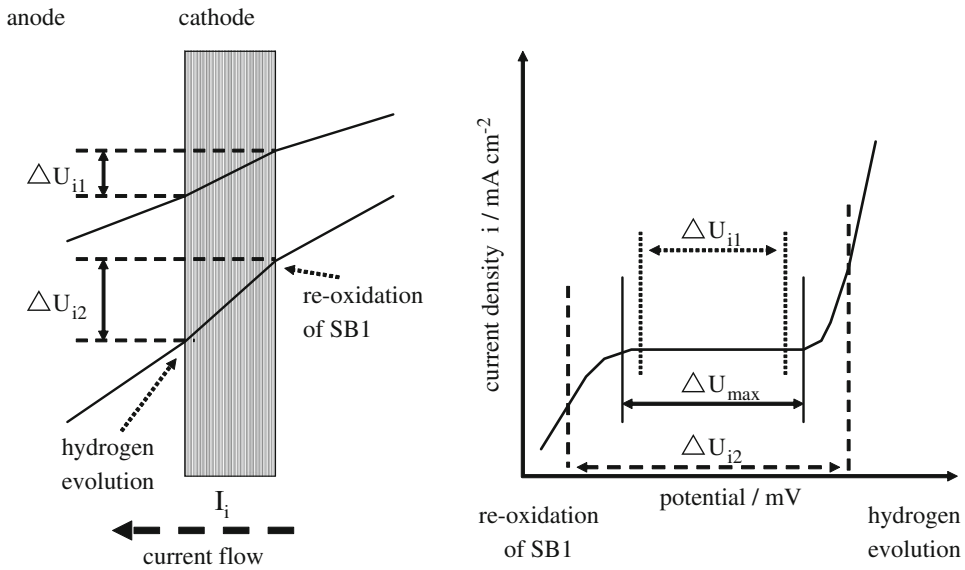

Fig. 2 Schematic representation of the voltage drop in catholyte and cathode, and voltammogram of SB1 in a flow cell. Reactions occur when voltage drop ΔU_i exceeds the length of the diffusion limited current plateau are indicated (ΔU_{i1} controlled cell operation, ΔU_{imax} maximum difference and ΔU_{i2} bipolar behaviour)

all electrodes are built with the same thickness, ΔU_i will be most critical for the cathode positioned next to the anode, because this cathode will exhibit bipolar reactions first.

In case of SB1 reduction, the value of ΔU_{max} depends on catholyte pH and cathode material used. For stainless steel cathodes and a catholyte containing 0.5 mol dm^{-3} NaOH the value for ΔU_{max} is 0.6 V [10]. At a cathode potential below −1,200 mV hydrogen evolution will occur, while at a cathode potential more positive than −600 mV reoxidation of the dyestuff and deposition of solid SB1 on the surface of the electrode will occur [10]. In case of SB1 reduction, ΔU_{max} of 0.6 V defines the maximum value of ΔU_i that must not be exceeded between front and rear of a porous three-dimensional electrode. In Ref. [34], ΔU_i has been related to geometric parameters of the cathode according Eq. 1.

$$\Delta U_i = I_i \frac{di}{\kappa A \omega} \cdot 10^5 \tag{1}$$

The potential drop ΔU_i depends on d_i the electrode thickness, I_i/A the charge density in the catholyte, κ the conductivity of the electrolyte and ω the porosity of the electrode. For a multi-cathode electrolyser built up of identical cathode units as shown in Fig. 1, the critical value ΔU_{max} will be reached first at the cathode nearest to the anode ($i = 1$). This electrode will define the maximum thickness of a three-dimensional cathode.

In the experimental example, a three-dimensional cathode was built up from L_i layers of stainless steel fabric with the geometric area A. The factor C_1 transfers the geometric area of the electrode into an electrode surface. For the fabric used the factor of 2.4 considers the surface of the wires used to weave an area A. With a given current density i_d, the current fed into a single three-dimensional electrode is calculated as the product $i_d A C_1 L_i \times 10^{-3}$. For an electrolyser with n cathodes, the current I_i transported in the electrolyte through the cathode in position i can be calculated according to (2).

$$I_i = i_d A C_1 L_i (n - i) \cdot 10^{-3} \tag{2}$$

Using woven steel fabric for electrode materials, the thickness d_i of a three-dimensional cathode can be transferred into a number of layers L_i according to (3). The factor C_2 corresponds to the thickness of the steel fabric used to build up the three-dimensional cathode stack. In plain weave fabric, the thickness of one layer fabric equals twice the diameter of the wires used, thus in the present case $C_2 = 0.04$ cm.

$$d_i = L_i C_2 \tag{3}$$

Combination of (1), (2) and (3) results in Eq. 4. When ΔU_{max} is used instead of ΔU_i and Eq. 4 is solved for L_i, the number of fabric layers L_i can be calculated as function material and process parameters.

$$L_i C_2 = \frac{\Delta U_i \kappa \omega}{i_d C_1 L_i (n - i) 100} \tag{4}$$

$$L_i = \sqrt{\frac{\Delta U_{max} \kappa \omega}{i_d (n - i) 100\ C_1 C_2}} \tag{5}$$

Equation 5 defines the maximum number of layers that can be combined to a cathode unit before bipolar behaviour will occur. L_i will be influenced by process conditions current density i_d, maximum permitted voltage difference ΔU_{max}, conductivity κ, cell parameters area A, electrode porosity ω and material properties C_1, C_2.

Theoretically each cathode unit of a multi-cathode electrolyser could be optimised individually, with the result

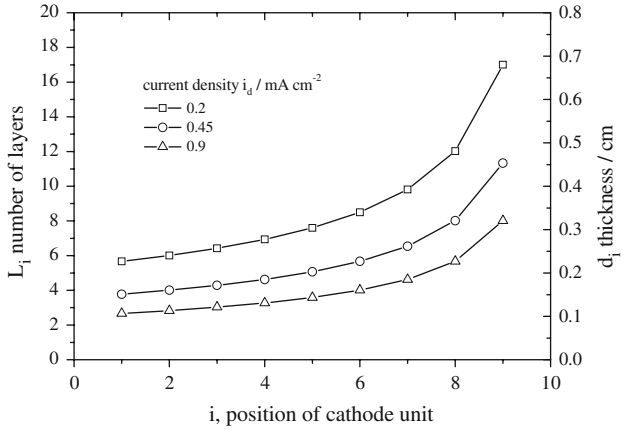

Fig. 3 d_i and L_i as a function of electrode position i 1–9 for a 10-cathode multi-electrode stack ($\Delta U_i = 0.6$ V, $\omega = 37\%$, $\kappa = 25$ mS cm^{-1}, $C_1 = 2.4$, $C_2 = 0.04$ cm and $A = 400$ cm^2) calculated for different current densities (*open square*) $i_d = 0.2$ mA cm^{-2}, (*open circle*) $i_d = 0.45$ mA cm^{-2} and (*open triangle*) $i_d = 0.9$ mA cm^{-2}, respectively

that cathodes nearer to the anode would require lower number of fabric layers than cathodes, which are positioned at higher distance from the anode. The maximum thickness of a cathode unit d_i and the number of layers L_i (for $C_2 = 0.04$ cm) can be calculated as a function of the electrode position i. Figure 3 presents values of d_i and L_i for the cathodes in a 10-cathode stack for different current densities i_d, as a function of electrode position.

In order to achieve the same current density i_d, this would also require a rather complicated current supply, because the cathode would have to be supplied with different currents I_i^*, dependent on the position of the cathode.

Thus, from technical point of view, production of a standardised electrode design is favourable.

When the same current is fed into each cathode unit, operating at current density i_d, the cell current I_c can be calculated from the area of a cathode unit A L_1 C_1 and the number of cathode units n. Equation 6 gives I_c as a function of current density and electrode geometry.

$$I_c = i_d A L_1 C_1 n \tag{6}$$

When the cathode stack is built up form identical units, the first electrode defines the critical limit for the thickness. In the example given, electrode thickness for a current density i_d of 0.2 mA cm^{-2} should be below 0.23 cm, with $L_1 = 5.7$. This means that the first three-dimensional cathode unit must be built up with a maximum of five layers of steel fabric. With increasing current density, the cathode thickness has to be decreased to 0.11 cm at $i_d = 0.9$ mA cm^{-2}, L_1 the number of fabric layers then has to be kept below a value of 2.7.

Increase in current density i_d permits to increase cell current, however, in addition, the thickness of electrodes also has to be reduced. For a cell operating near the current limit for bipolar behaviour, total cell current I_c cannot be increased in proportion with current density i_d, because L_i has to be decreased at the same time.

Equation 6 can be used to calculate the cell current I_c for the examples given in Fig. 3. For a current density of 0.2 mA cm^{-2}, the cell current I_c is 9.6 A, which increases to 17.3 A at i_d 0.9 mA cm^{-2}. An increase in current density i_d from 0.2 mA cm^{-2} to 0.9 mA cm^{-2} corresponds to a factor of 4.5; however, I_c can be increased only by a factor of 1.8.

For a given current density i_d, I_c can be increased with higher number of cathodes, however, I_c cannot be increased linearly with electrode number, because at the same time thickness d_i has to be reduced to hold ΔU_i below the critical limit.

In the given example for cathode in position $i = 10$, Eq. 9 does not define a limiting thickness d_i, because the current transported through the porous electrode I_{10} is zero. Increase in cathode thickness, however, does not imply that every point of the three-dimensional cathode will work with the same current density i_d. For this electrode, model designs for current density distribution in three-dimensional electrodes can be applied following to the literature [15–20, 24–32].

Electrolyte conductivity also determines the maximum electrode thickness d_i, and thus, the cell current I_c (Eq. 5). The influence of electrolyte conductivity κ on the design of the electrolyser is shown in Fig. 4. Increasing electrolyte conductivity κ results in decreased voltage drop in the cathode unit ΔU_i, thus thicker cathode units can be used. As a result, for a given current density i_d, an increase in

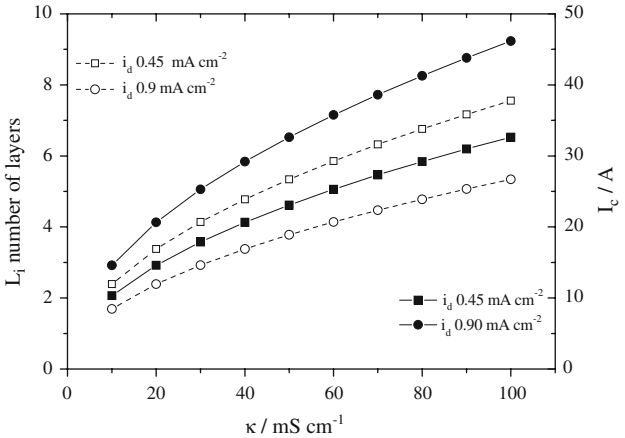

Fig. 4 Electrode thickness d_i and total cell I_c current for a 10-electrode multi-cathode electrolyser as a function of catholyte conductivity κ calculated for two current densities i_d; $i_d = 0.45$ mA cm^{-2} (*filled square*) cell current I_c, (*open square*) number of layers; $i_d = 0.9$ mA cm^{-2} (*filled circle*) cell current I_c, (*open circle*) number of layers ($\Delta U_i = 0.6$ V, $\omega = 37\%$, $\kappa = 10$–100 mS cm^{-1}, $C_1 = 2.4$, $C_2 = 0.04$ cm and $A = 400$ cm^2)

conductivity permits higher cell currents I_c. For example, at a conductivity of $\kappa = 10$ mS cm^{-1} and current density $i_d = 0.45$ mA cm^{-2} a two layered cathode can be used ($L_1 = 2$, $I_c = 8.6$ A). With $\kappa = 100$ mS cm^{-1}, the electrode thickness can be increased to seven layers and I_c increases to 30.2 A.

3.2 Model calculations of cell voltage

The variation of cell voltage $U_1 - U_n$ of a multi-cathode electrolyser is of relevance for the design of a cost effective power supply and for estimation of energy consumption. Thus, a model to estimate the cell voltage from a set of experimental data would be a useful tool. For the calculation of U_i, the cell voltage of an individual electrode in a multi-cathode electrolyser, we can use the model of a network of resistors, representing the different elements of the cell (Fig. 5).

R_0 includes the electric resistance of catholyte between cathode and separator, cation-exchange membrane, anolyte and also includes contributions of anode reaction and anodic overvoltage. R_z represents the ohmic resistance of the cathode material and includes the contribution of cathode reaction and cathodic overvoltage. R_i stands for the electrical resistance between two neighbouring cathode units, which depends on the geometric distance between the cathode units, the porosity of the insulation material separating the electrodes, and the conductivity of the catholyte. R_i also includes the electrolyte resistance for charge transport through the porous three-dimensional cathode to the front of a given cathode.

In the example shown, the total cell current I_c is distributed equally to the n cathode units each supplied with current I_n^* (Eq. 7). The cell voltage of cathode unit 2 can be calculated according to Eq. 8 and the cell voltage of electrode i is calculated according to Eq. 9. Equation 9 can be transformed into a general description of the cell voltage U_i of a cathode unit in position i (Eq. 10).

$$I_c = nI_n^* \quad I_1^* = I_2^* = I_n^* \tag{7}$$

$$U_2 = I_cR_0 + R_zI_n^* + R_1\left(I_c - I_n^*\right) \tag{8}$$

$$U_i = I_cR_0 + R_zI_n^* + R_i\sum_{j=1}^{i}\left(I_c - (j-1)I_n^*\right) \tag{9}$$

$$U_i = I_cR_0 + R_zI_n^* + (i-1)R_iI_c - R_iI_n^*(i-1)i/2 \tag{10}$$

$$U_n = I_cR_0 + R_zI_n^* + (n-1)R_iI_c - R_iI_n^*(n-1)n/2 \tag{11}$$

$$U_n = R_{cell}I_c + (n-1)R_iI_c - R_iI_n^*(n-1)n/2 \tag{12}$$

The cell voltage of electrode n is given by Eq. 11. The contribution of cell resistance R_0 and cathode resistance R_z both are independent of the electrode position. Replacing I_n^* by I_c/n, the term $I_cR_0 + R_zI_n^*$ can be combined to the term R_{cell} I_c (Eq. 12). Equations 10 and 12 permit the calculation of the cell voltage of a multi-cathode electrolyser for different cell current. R_{cell} and R_i can be determined from fitting of theoretical curves to experimental values.

In Fig. 6, the experimental cell voltages U_i measured during cathodic reduction in experiment nos. V1, V3, V4 and V5 and calculated data using Eq. 12 are shown. Deviation in individual experimental points from the theoretical graphs are due to the manual adjustment of the power supplies. In Table 3, relevant values for R_{cell} and R_i used in the model calculations are given. Experimental conditions given were determined at the time of cell voltage measurements.

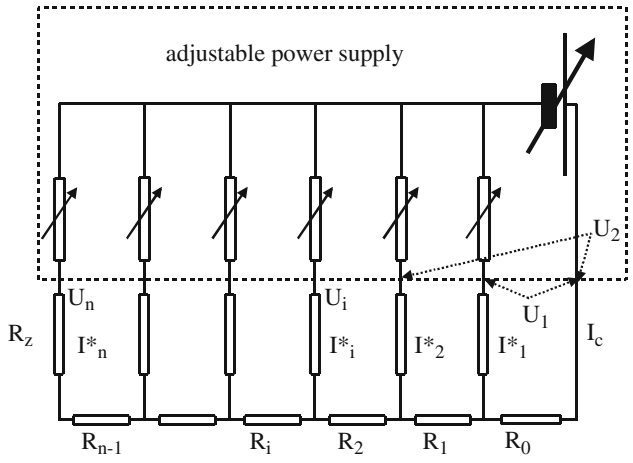

Fig. 5 Resistor network used to calculate individual cell voltages of cathode units U_i

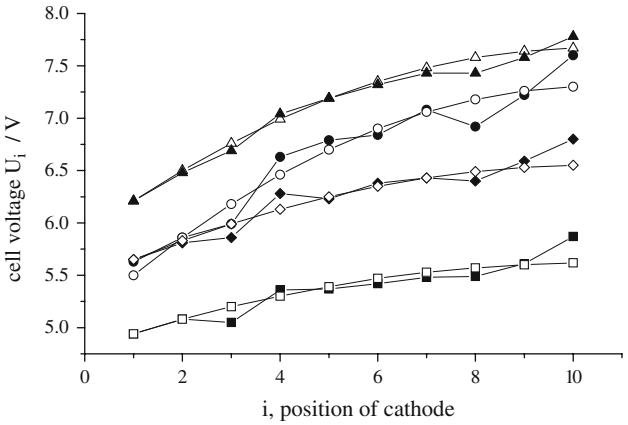

Fig. 6 Experimental cell voltage and calculated data for electrolysis experiments: (*filled circle*) V1 $I_c = 10$ A, $n = 10$, $R_{fix} = 0.55$ Ω, $R_i = 0.040$ Ω; (*open circle*) calculated data for 10 A; (*filled triangle*) V3 $I_c = 5$ A, $n = 10$, $R_{fix} = 1.24$ Ω, $R_i = 0.063$ Ω; (*open triangle*) calculated data for 5 A; (*filled diamond*) V4 $I_c = 10$ A, $n = 10$, $R_{fix} = 0.57$ Ω, $R_i = 0.020$ Ω; (*open diamond*) calculated data for 10 A; (*filled square*) V5 $I_c = 10$, $n = 10$, $R_{fix} = 0.50$ Ω, $R_i = 0.015$ Ω, (*open square*) calculated data for 10 A

Table 3 R_i and R_{cell} used for cell voltage calculations shown in Fig. 6 and relevant experimental conditions when experimental cell voltage values were measured

No.	I_c (A)	R_{cell} (Ω)	R_i (Ω)	SB1 crude (g kg^{-1})	SB1 dry (g kg^{-1})	Q (A min)	Q_{spez} (A min kg^{-1})	T (°C)
V1	10	0.550	0.040	80	51.0	3600	360	34
V3	5	1.242	0.063	141	90	875	250	29
V4	10	0.565	0.02	118	70.7	3450	761	32
V5	10	0.494	0.015	459	292	8425	1520	28

The values for R_{cell} depend on both the conductivity of catholyte and anolyte. For V1, V4 and V5, the value for R_{cell} was calculated with approximately 0.5 Ω, while for V3 the value for R_{cell} was determined with 1.2 Ω.

Values for R_i range from 0.015 Ω to 0.05 Ω. Experiment V3 was run with a reduced catholyte volume. Thus, the higher values for R_{cell} and R_i both are due to the lower electrolyte level in the cell (Table 2).

For a given cell construction, variation of R_i mainly depends on the catholyte conductivity. The variation of R_i cannot be explained by the differences in dyestuff concentration or catholyte temperature, but clearly depends on Q_{spez} the charge flow applied per kg of catholyte. Dependent on Q_{spez}, the electrolyte concentration in the catholyte increases and R_i decreases.

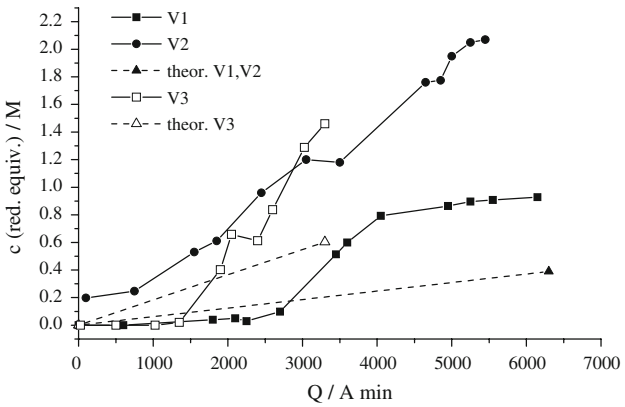

Fig. 7 Concentration of reducing equivalents as a function of charge flow for experiments (*filled square*) V1 (*filled circle*) V2 and (*filled triangle*) calculated value for V1 and V2; (*open square*) V3 and (*open triangle*) calculated value for V3

3.3 Cathodic dyestuff reduction

Electrolysis was started with a catholyte volume given in Table 2. Insoluble SB1 then was added in small portions to avoid plugging of the three-dimensional cathode by high concentration of dispersed dyestuff.

With start of current flow, the redox potential in the catholyte lowers from initially −205 mV to more negative values. During the initial phase of electrolysis, a small amount of dispersed SB1 has to be reduced by direct cathodic reduction [1, 12, 13].

When reduced SB1 has been formed in the catholyte these dissolved molecules can take over the function of a soluble mediator. The main cathode reaction then is indirect cathodic reduction of dispersed SB1 using the Leuco form of SB1 as reversible redox mediator. Experimental conditions of the electrolysis experiments are given in Table 2. The NaOH concentration in the catholyte at the end of the electrolysis has been calculated from the total charge flow and has been related to the initial volume of catholyte.

The increase of reducing equivalents in the catholyte as a function of charge flow is shown in Fig. 7.

In experiment V1 51 g kg^{-1} SB1 were used, while in experiment V2 the final concentration of SB1 reached 102 g kg^{-1}. As expected, in V2 the concentration of reducing equivalents in the catholyte reached almost double the value of experiment V1 (Fig. 7).

In V3, an amount of 252 g kg^{-1} crude SB1 was added to the catholyte during the first 7 h of electrolysis at 5 A cell current, then electrolysis was continued for 4 h at 5 A. Due to the low total charge flow and the high concentration of dyestuff, dyestuff reduction was not complete in V3 after an electrolysis time of 11 h. This explanation is also supported by the less negative redox potential measured in the catholyte at the end of experiment V3. While in V1, V2 and V4, the final redox potential in the catholyte was between −599 mV and −618 mV, in V3 a potential of only −521 mV was registered at the end of the electrolysis.

In Fig. 7, dashed lines indicate the theoretical build up of reducing equivalents in the catholyte according to Faraday's law. For all experiments shown, the analytical results exceed the theoretical lines with progress of time. From the synthesis, SB1 is released in reduced form, which is then oxidised and filtered off. During oxidation and precipitation of the dyestuff partly oxidised dyestuff is enclosed in the precipitate. As a result of the electrochemical reduction these partly reduced molecules are released into the catholyte, which explains the unexpectedly high concentration of reducing equivalents found in the catholyte [12, 13].

3.4 Formation of a highly concentrated product

In order to achieve a product with commercial value, the reduction of SB1 should yield a highly concentrated solution. In prolongation of V4, a further amount of crude SB1

was added and reduced cathodically. Finally, a mass of 4,789 g crude SB1 had been added to the initial volume of 4 kg water. The liquid product released at the end of the electrolysis contained 61.45% w/w crude SB1 and 36.9% w/w dry SB1.

The total mass of electrolyte and added SB1 was 8,789 g. At the end of the experiment, the total mass of product was weighed at 9,629 g. Thus, a mass of 840 g had been transported through the cation-exchange membrane because the Na^+-ion transport and accompanied hydration water.

A charge flow of 298.5 Ah had been used to reduce 4,789 g crude SB1 (2,873 g dry dyestuff), which corresponds to 11.1 moles Na^+-ions, which had passed through the membrane into the catholyte. When an associated transport of 3–4 water molecules is considered for each Na^+-ion, 11.1 moles of Na^+-ions will correspond to a total mass of 256 g Na^+-ions and 599–799 g hydrate water.

The results show that for the technical scale production of concentrated SB1 solutions indirect dilution by hydrate water coupled to the Na^+-transport has to be considered.

3.5 Savings

An estimation of chemical savings can be made on basis of the charge flow required to reduce a certain amount of SB1. In experiment V3, 0.644 kg dry SB1 was reduced by a charge flow of 57.5 Ah at a voltage of maximum 7.5 V. This corresponds to an amount of 3.33 mol reducing equivalents per 1 kg dry SB1 and to an energy consumption of 0.67 kWh/kg dry SB1 filter cake. When sulphide reducing agents are used instead of cathodic reduction the amount of Na_2S can be calculated from Eq. 13.

$$Na_2S \rightleftarrows 2\,Na^+ + 1/xS_x + 2e^- \qquad (13)$$

According to Faraday's law 3.33 moles equal an amount of 129 g Na_2S, which will be required to reduce 1 kg of dry SB1 filter cake.

3.6 Dyeing experiments

In order to study the dyeing behaviour of cathodically reduced SB1, exhaust dyeing experiments on cotton fabric were compared to reference dyeings with commercial C.I. Sulphur Black 1 (Cassulfon® Carbon CMR). Due to the rather undefined chemical composition of C.I. Sulphur Black 1, an analytical determination of dyestuff concentration in a concentrated product is difficult. The usual procedure for an assessment of a product quality is to compare shade and colour depth of dyeings. A series of dyeing experiments with cathodically reduced SB1 and a commercial quality SB1 was performed. The CIELab coordinates of the dyeings are shown in Table 4.

Table 4 CIELab coordinates of dyeings with cathodically reduced dye and reference dyeings (ref = dyeing used as reference sample)

Sample No	Dyestuff	Concentration (g dm^{-3})	Average			ΔE
			L*	a*	b*	
1	CMR	10	13.24	−3.82	−3.39	
2	CMR	15	12.31	−3.62	−2.95	Ref
3	V4	10	12.75	−3.58	−3.69	0.864
4	V4	15	11.95	−3.44	−2.63	0.422
5	V4	20	11.51	−3.29	−2.63	–
6	V4	25	11.34	−3.12	−2.57	–

ΔE = CIELab total colour difference

Colour depth and shade given as L^*, a^* and b^*-coordinates, of reference dyeings with use of 15 g dm^{-3} Cassulfon Carbon® CMR (sample 2) are similar to dyeings with 10 and 15 g dm^{-3} cathodically reduced SB1 (samples 3 and 4). The total colour difference ΔE was calculated according to Eq. 14.

$$\Delta E = \sqrt{(\Delta L^*)^2 + (\Delta a^*)^2 + (\Delta b^*)^2} \qquad (14)$$

Total colour difference between samples 2 and 3 was determined at $\Delta E = 0.864$ and between samples 2 and 4, a value of $\Delta E = 0.422$ was obtained. In practice of colour measurement, a value for the total colour difference ΔE below 1 is acceptable. Sample 3, dyed with 10 g dm^{-3} dyestuff solution was found to be slightly lighter (higher L^* value), and the dyeing 4 obtained with 15 g dm^{-3} dyestuff solution appeared darker (lower L^* value) than the reference dyeing with 15 g dm^{-3} commercial product (sample 2). For both cases, the value for ΔE is below 1, which confirms that under the conditions used in this study, dyeing behaviour of the SB1 is independent of the reduction method.

4 Conclusions

Multi-cathode electrolysers represent a promising cell concept for electrolysers designed to operate at low current densities.

At high cell current the first electrodes of multi-cathode electrolysers are at risk to show bipolar reactions. The rear face of a cathode then exhibits anodic dyestuff oxidation, while cathodic water reduction is observed at the front side. For a given electrode thickness d_i, a critical limit with regard to the maximum cell current I_i transported in the electrolyte through the porous three-dimensional cathode exists. Existing concepts for three-dimensional electrodes are useful for the estimation of the thickness of a single three-dimensional electrode. The model calculations given in this article help to identify critical limits when

three-dimensional electrodes are combined to a multi-cathode electrolyser and where the charge flow transported in the electrolyte through a porous electrode exceeds by far the current of the respective electrode.

Using a simple mathematical model for the cell permits estimation of the maximum thickness of a three-dimensional cathode element, for given experimental conditions and electrode construction, e.g. type of steel fabric used as cathode material.

The results demonstrate limitations for an increase in cell current of a multi-cathode electrolyser by increasing the number of cathodes used. For example, doubling the number of isolated cathode units in a multi-cathode stack does not permit the same increase in cell current, because cathode thickness has to be reduced to avoid bipolar behaviour.

However, the calculations also demonstrate the significant potential of multi-cathode electrolysers to reach high cell currents I_c with electrolytes, that allow only low current densities.

The cell voltage of individual cathodes in a multi-cathode electrolyser can be described by a resistor network. Once R_{cell} and R_i have been determined for a certain application, an optimisation of a cell construction with regard to cell design and energy consumption can be done.

The presented mathematical models permit an optimisation of electrode number, electrode thickness and cell voltage for a certain technical application.

The cathodic reduction of C.I. Sulphur Black 1 can be performed in multi-cathode cells equipped with three-dimensional electrodes. Obtained solutions with high dyestuff content can be used as commercial product. The dyeing behaviour of the cathodically reduced product SB1 was found to be comparable to dyeing results with commercial samples of SB1.

In order to obtain dyestuff formulations with high concentration, the water brought into the catholyte by the wet filter cake and by hydrate water transport through the cation-exchange membrane has to be reduced to a minimum.

Acknowledgements Authors thank the DyStar Textilfarben GmbH (Frankfurt, Germany) for supplying material, technical discussion and assistance.

References

1. Bechtold T, Berktold F, Turcanu A (2000) J Soc Dyers Color 116:215
2. Heid C, Holoubek K, Klein R (1973) Melliand Textilber 12:1314
3. Aspland JR (1992) Textile Chem Color 24(3):21
4. Aspland JR (1992) Textile Chem Color 24/4:27
5. Hähnke M (1995) Melliand Textilber 76:414
6. Nowack N, Brocher H, Gering U, Stockhorst T (1982) Melliand Textilber 63:134
7. Blackburn RS, Harvey A (2004) Environ Sci Technol 38:4034
8. Frind H, Held C, Aman H (1969) Ger Offen 1:906083
9. Bechtold T, Brunner H (2005) Electrochemical processes in textile processing. In: Nuñez M, (ed) New developments in electrochemistry research, Chap. 1. Nova Science Publishers, NY, pp. 1–55 (ISBN 1–59454-544–8)
10. Bechtold T, Burtscher E, Turcanu A (1998) J Appl Electrochem 28:1243
11. Bechtold T, Burtscher E, Turcanu A, Bobleter O (1998) Text Chem Color 30/8:72
12. Bechtold T, Turcanu A, Schrott W (2008) J Appl Electrochem 38:25
13. Bechtold T, Turcanu A, Schrott W (2008) Dyes Pigments 77:502
14. Bechtold T, Turcanu A, Burtscher E, Bobleter O (1997) Textilveredlung 32:204
15. Kreysa G (1978) Chem-Ing-Tech 50:332
16. Kreysa Ber G (1988) Bunsenges Phys Chem 92:1194
17. Kreysa G (1976) Chem-Ing-Tech 48:852
18. Polcaro AM, Palmas S, Renoldi F, Mascia M (2001) Electrochimica Acta 46:389
19. Jüttner K, Galla U, Schmieder H (2000) Electrochimica Acta 45:2575
20. Jüttner K (2007) Technical scale of electrochemistry, in encyclopaedia of electrochemistry. In: Bard AJ, Stratmann M (eds) Electrochemical engineering, vol 5. Wiley, Weinheim, Germany ISBN: 978-3-527-30397-7
21. Hu XE, Yang HW, Wang XJ, Bai RS (2002) J Appl Electrochem 32/2:321
22. Tissot P, Fragniere M (1994) J Appl Electrochem 24/6:509
23. Zhou M, Gu H, Lei L (2005) Groundwater remediation by three dimensional electrode biofilm reactor. Proceedings of the 9th International Conference on Environmental Science and Technology, Rhodes island, Greece, 1–3 September 2005
24. Newman JS, Tobias CW (1962) J Electrochem Soc 109:1183
25. Heitz E, Kreysa G (1986) Principles of electrochemical engineering: extended version of a DECHEMA experimental course. VCH Verlagsges, mbH, Weinheim, p 127 ISBN 3-527-25985-6
26. Prentice G (1991) Electrochemical engineering principles. Prentice-Hall International, New Jersey ISBN 0-13-248881-7 Inc
27. Alkire R, Ng PK (1974) J Electrochem Soc 122:95
28. Stankovic VD, Grujic R, Wragg AA (1998) J Appl Electrochem 28/3:321
29. Stankovic VD, Wragg AA (1995) J Appl Electrochem 25/6:565
30. Stankovic VD, Lazarevic G, Wragg AA (1995) J Appl Electrochem 25/9:864
31. Stankovic VD, Wragg AA (1984) J Appl Electrochem 14/5:615
32. Li J, Hu X, Su Y, Li Q (2007) Chem Eng Sci 62:6784
33. Masliy AI, Poddubny NP (1998) Electrochim Acta 43:599
34. Bechtold T, Burtscher E, Bobleter O, Blatt W, Schneider L (1998) Chem Eng Tech 21:877
35. Vallières C, Matlosz M (1999) J Electrochem Soc 146/8:2933
36. Bechtold T, Turcanu A (2002) J Electrochem Soc 149:D7
37. Hinman AS, Wiebe P (1995) Anal Chem 67/4:694
38. Hingman AS, Tang C (1991) Electrochim Acta 36(5–6):841
39. Förster HJ, Thiele W, Kramer HJ, Brunner H, Schrott W, Bechtold T (2004) Patent Application Elektrolysezelle mit Mehrlagen-Streckmetallelektroden, 7.5.2004, DE 10 2004 023 161 A1, Electrolytic cell comprising multilayer expanded metal EP2005004838, USPTO Patent Application 20080245662
40. Sakakibara Y, Nakayama T (2001) Water Res 35/3:768
41. Lenard DR, Schattschneider GK, Moores GJ (1993) Br Corros J 28/4:259
42. Yarnitzky CH, Ariel M, Zur C (1980) J Appl Electrochem 10/4:473
43. Blatt W, Schneider L (1999) Melliand Int 80:240